Frequency-Based Current-Sharing Techniques for Paralleled Power Converters

David J. Perreault Robert L. Selders, Jr. John G. Kassakian

Massachusetts Institute of Technology
Laboratory for Electromagnetic and Electronic Systems
Cambridge, MA 02139 USA

Abstract - This paper introduces a new current-sharing technique for paralleled power converters which is based on frequency encoding of the current-sharing information. The approach has significant advantages over existing methods, including the ability to transformer isolate or eliminate current-sharing control connections. Operation of the current-sharing technique is analyzed, and experimental results from a 3-cell prototype system are presented.

I. Introduction

Power conversion systems are sometimes constructed by paralleling converters in order to improve performance or reliability, or to attain a high system rating. A desirable characteristic of a parallel converter architecture is that the individual converters share the load current equally and stably. The current-sharing behavior of the system is largely dependent on the manner in which the individual converters are controlled. Many parallel converter systems use some form of global control, in which a single, possibly redundant, controller directly regulates the load balance among the individual converters [1-8]. However, to enhance modularity and improve reliability, it is more desirable to have the load-sharing control distributed among the converters. This is especially true in *cellular* converter architectures, in which large numbers of quasi-autonomous converters, called *cells*, are paralleled to form a large power converter [9-11].

In order to implement a distributed load-sharing scheme, only a very limited amount of information needs to be shared among the individual cells. For example, given information about the average cell output current, each cell can regulate its output to be close to the average [12-17]. Other quantities valid for the ensemble of converter cells can also be used, including rms cell current [18], weighted cell current stress [19], and highest cell current [20].

Load-sharing information is most commonly generated and shared over a single interconnection among converter cells. Typically, the interconnection circuit is designed so that when each cell generates a signal proportional to its output, the voltage on the interconnection bus is the average (or maximum, etc.) of the individual signals. For ac output converters, the interconnection may sometimes be transformer isolated from the local cell control circuits [12,13]. However, for many applications transformer isolation cannot be employed using conventional methods, since the current-sharing information has frequency content down to dc.

Approaches exist where current-sharing information is communicated implicitly via the output, and no additional interconnections among converter cells are required. For paralleled constant-frequency inverters, load balance can be achieved by implementing a frequency and voltage droop characteristic in each cell output. This technique, which is also used to regulate the power output of paralleled generators in an ac supply system, basically employs the ac bus voltage and frequency to communicate power-sharing information among the controllers [13,21]. Unfortunately, the complexity and cost of the approach limits its use to relatively large inverter cells. Dc output supplies sometimes use output voltage droop characteristics to achieve a degree of current-sharing [22,23]. While simple, this approach yields heavy load regulation in the output and steady-state current imbalances, which are often unacceptable.

This paper introduces a new, frequency domain based method for encoding and distributing current-sharing information among cells. This new scheme has significant advantages over existing methods, particularly with respect to reliability. It operates in the following manner. Each converter cell generates a (typically sinusoidal) signal whose frequency is related to the average output current (or power or other variable to be regulated) of the cell. The frequency range used can be widely separated from the fundamental output frequency of the converter system. The signals from each cell are summed, with the result available to each cell. Each cell employs a frequency estimator circuit to calculate a weighted average, ω_{est}, of the frequency content of the aggregate signal. Each cell can then compare its own generated frequency, ω_k, to the weighted average ω_{est}, and adjust its output to make $\omega_k \simeq \omega_{est}$. With this method, a priori information about the number of cells in a paralleled system is unnecessary, since each cell needs only the aggregate signal for current sharing to be effected.

This frequency encoding approach circumvents some of the major limitations of existing current-sharing methods. The direct interconnection among control circuits present in conventional distributed load-sharing schemes is a source of single-point failure mechanisms which, in the worst case, can bring the entire converter system down. Elimination of single-point failure modes is a key design objective for achieving fault tolerance in distributed converter architectures [24]. We will show that with the frequency-based approach, current-sharing information can be encoded at high frequencies and distributed over the output or input bus, making additional interconnections among cells for

0-7803-3500-7/96/$ 5.00 © 1996 IEEE

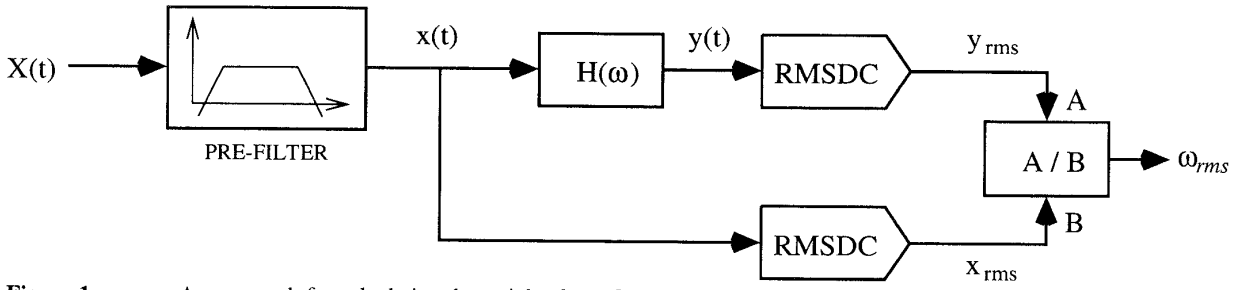

Figure 1 An approach for calculating the weighted rms frequency estimate of the aggregate signal. This approach is easily implemented in analog or digital hardware.

current sharing unnecessary. Alternatively, if separate interconnections for current-sharing are used, they may be galvanically isolated using small, high-frequency transformers. Thus, the frequency encoding method thus allows improvements in reliability and availability by eliminating the failure modes associated with direct interconnections among the control circuits.

This new control design has other potential advantages. In conventional schemes, current-sharing information is encoded and distributed at low frequencies (typically down to dc). With the frequency-encoding approach, the designer can select the frequency range over which current-sharing information is communicated, and can use this design freedom to achieve objectives such as noise minimization. Furthermore, because the current-sharing information can be directly communicated over the input or output bus with this method, the dedicated interconnections for communicating this information can be eliminated if desired. Finally, with the frequency-based method, the aggregate current-sharing signal contains information about the total number of converter cells and their *individual* output currents in addition to information about the average output of the converters. This may have some benefits for system monitoring and fault detection.

II. Frequency Estimation

To reduce this new current-sharing approach to practice, a means of estimating an average frequency ω_{est} from the aggregate signal using simple, inexpensive circuitry is needed. Many different types of weighted estimates and estimator structures are possible. This section considers the implementation of an rms frequency estimator, though other frequency-based estimation and control schemes exist which are also well suited to the task.

Consider the aggregate current-sharing signal $x(t)$, which is made up of a group of N sinusoids $x_k(t)$ of frequencies ω_k, $k = 1,.., N$. The frequency of an individual sinusoid encodes information about the output current of a particular cell, while the rms frequency of the aggregate signal can be used to effect current-balancing control. The weighted rms frequency for all of the sinusoids is defined as:

$$\omega_{rms} = \frac{\sqrt{\sum_{k=1}^{N} c_k^2 \omega_k^2}}{\sqrt{\sum_{k=1}^{N} c_k^2}} \tag{1}$$

where the c_k's are weighting coefficients for different frequencies. For equal weighting, the c_k's can be considered equal to a single (arbitrary) constant. The power spectrum of $x(t)$ is:

$$S_x(\omega) = 2\pi \sum_{k=1}^{N} \frac{1}{2} |X_k|^2 [\delta(\omega - \omega_k) + \delta(\omega + \omega_k)] \tag{2}$$

where we have assumed that all of the $x_k(t)$'s are at separate frequencies. The violation of this assumption affects the weightings in the rms frequency estimate, but does not interfere with the overall operation of the current-sharing system. The rms value of x is then:

$$x_{rms} = \sqrt{\frac{1}{2\pi} \int_{-\infty}^{+\infty} S_x(\omega) d\omega} = \sqrt{\sum_{k=1}^{N} |X_k|^2} \tag{3}$$

If we pass the signal $x(t)$ through a filter with frequency response $H(\omega)$ to form a signal $y(t)$, we find the new signal $y(t)$ has the properties

$$S_y(\omega) = 2\pi \sum_{k=1}^{N} \frac{1}{2} |H(\omega_k)|^2 |X_k|^2 \cdot [\delta(\omega - \omega_k) + \delta(\omega + \omega_k)] \tag{4}$$

and

$$y_{rms} = \sqrt{\frac{1}{2\pi} \int_{-\infty}^{+\infty} S_y(\omega) d\omega} = \sqrt{\sum_{k=1}^{N} |H(\omega_k)|^2 |X_k|^2} . \tag{5}$$

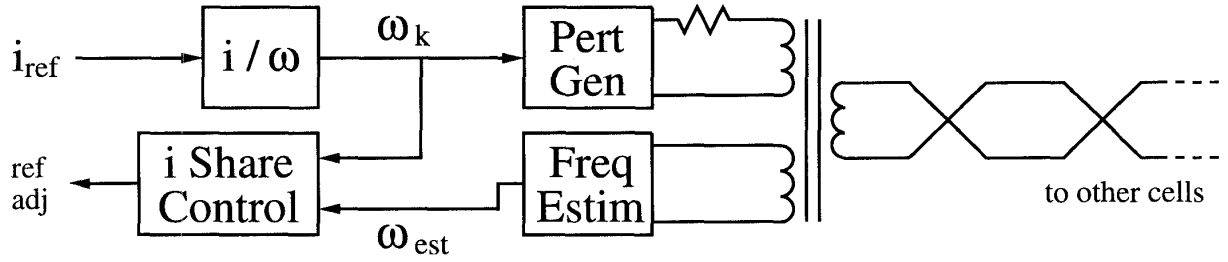

Figure 2 Schematic of the isolated single connection implementation of frequency-based load-sharing control.

Now consider the estimator implementation shown in Fig. 1. If we choose the filter be a differentiator over the encoding frequency range ($H(\omega) = j\omega$), we find that the ratio of the rms value of $y(t)$ to the rms value of $x(t)$ has the form of the desired rms frequency estimate (**1**), with the signal magnitudes as the weighting coefficients. This result means that the desired rms frequency estimate can be easily computed using simple analog or digital hardware.

The estimate can be calculated with analog circuitry using two (integrated circuit) rms-to-dc converters, a differentiator, and a divider. Alternately, the estimate can be computed digitally by sampling $x(t)$ and performing the equivalent calculations in software. These results have been derived for computations on fixed-frequency signals over all time. However, computation of these rms quantities over a sliding window allows the frequency content (and hence the current-balance information) to be tracked over time. Appendix A addresses the use of practical rms-to-dc converters for this purpose, and shows the effects of the averaging time constant of the rms-to-dc converters on frequency resolution and response speed.

We conclude from these results that if the individual cells encode information about their output current in the frequency of a signal, then information about the average output of all the cells can be easily extracted from the aggregate signal with very simple hardware. We now employ these results to implement the new frequency-based current-sharing scheme.

III. Implementation Approaches

To implement load-sharing control using the frequency encoding method, the signals from the individual cells are summed at a node, and the resulting aggregate signal is accessible to all the cells. There are several possible methods for doing this, each with its own attributes. We will consider three alternative implementation approaches for frequency-based current sharing, each with its own attributes: the isolated single connection implementation, the output perturbation implementation, and the switching ripple implementation.

The Isolated Single Connection Implementation

The *isolated single connection implementation* communicates current-sharing information over a dedicated bus, similar to existing single connection approaches [12-17,19,20]. Each converter cell injects onto the current-sharing bus a signal whose frequency is related to its output current. The cell measures the aggregate signal on the bus to determine ω_{est}, and control current balance (Fig. 2). Transformer isolation can be employed because there is no low-frequency content to the current-sharing signals. The ability to employ transformer isolation is an advantage over existing methods because it reduces the possibility that a single-point failure can damage the whole system via the current-sharing connections. Furthermore, this approach is advantageous for systems in which the converter control circuits do not share a common ground, such as isolated converter cells supplied from different power sources.

The Output Perturbation Implementation

The *output perturbation implementation* uses small sinusoidal perturbations in the cell output currents to encode current-sharing information (Fig. 3). Each cell computes an estimate (using the same method as the isolated single connection implementation) of the average output of all cells from the resulting aggregate perturbation in output voltage, which is locally measurable by each cell. This information is then used to achieve load balance among cells. The perturbation frequency range is typically selected to be well above the output voltage control bandwidth of the system, but well below the switching frequency. The needed perturbations in output current are easily generated in converters under current-mode control, and only very small perturbations in output current (and voltage) are necessary to communicate current-sharing information. The output perturbation implementation achieves current balance control using only variables measured locally at each converter cell, with no inter-cell connections for current-sharing. No additional power processing components or sensors are needed to communicate the current-sharing information across the output bus. This yields a potential reliability advantage over systems which utilize additional interconnections.

The use of the output bus to communicate current-sharing information has other interesting characteristics. For example, conditions which disrupt the distribution of current-sharing information (such as output short circuits) generally cause enough

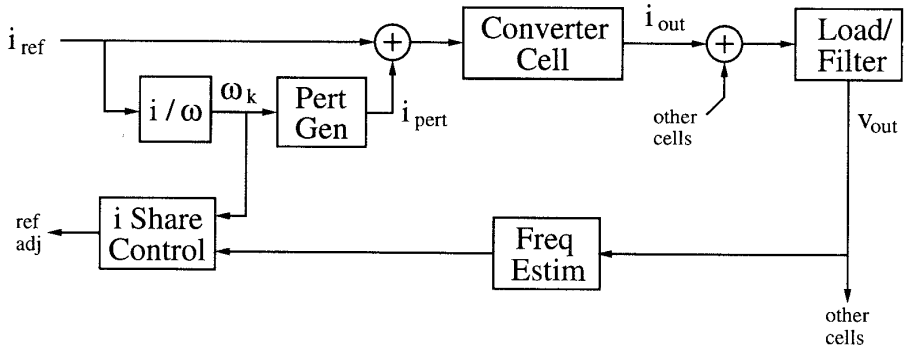

Figure 3 Schematic of the output perturbation implementation of frequency-based load-sharing control.

of a voltage error to drive all of the converters to full current, making current-sharing temporarily unnecessary. Furthermore, faults in an individual cell which cause it to be removed from operation (such as by the output fuse blowing) automatically prevent it from affecting current sharing among the remaining converter cells. These facts result in a current-sharing approach which is potentially very robust. The major challenge to implementing the approach is the selection of an appropriate perturbation magnitude and frequency range.

The Switching Ripple Implementation

The *switching ripple implementation* is similar to the output perturbation method, except that the switching ripple of the cell is used as the perturbation source (Fig. 4). Each converter cell is controlled such that its average output current (or some other variable to be regulated) is directly related to its switching frequency. Each converter can locally measure the aggregate switching harmonics at the output, and use the information in the switching harmonics to achieve load balance with the other converter cells. This approach has the benefit that no additional ripple is injected into the output to encode current sharing information, and the information is communicated at the switching frequency (i.e., with high bandwidth).

Controlling the switching frequency of the converters is typically straightforward. For many converter types, there is a natural relation between switching frequency and control variables such as output current. Converter control strategies which do not exhibit such a relation can often be modified to achieve it. For example, such a relationship can be implemented in fixed-frequency PWM converters by modifying the clock frequency as a function of output current.

Estimating an average value for the current (or frequency, or other control variable) from the aggregated output harmonics is a more delicate task. Because the switching harmonic content of a single converter operating at any frequency/current is known, information about the average can clearly be extracted from the output voltage. However, the existence of (possibly large) harmonics of the fundamental ripple current from each cell complicates the estimation task as compared to the output perturbation method. Nevertheless, we have managed to verify that for some converter types it is possible to estimate the rms output current directly from the net switching ripple using only locally measurable variables[25]. Furthermore, some very simple estimation and control structures exist which are insensitive to harmonic components, and are thus well suited to the switching-ripple implementation.

IV. Experimental Results

A low-power 3-cell prototype converter system implementing the output perturbation implementation was constructed. It will be demonstrated that, using perturbations in the output voltage of less than one percent, current sharing accurate to a few percent can be achieved with no control interconnections among cells.

The prototype system is composed of buck converter cells

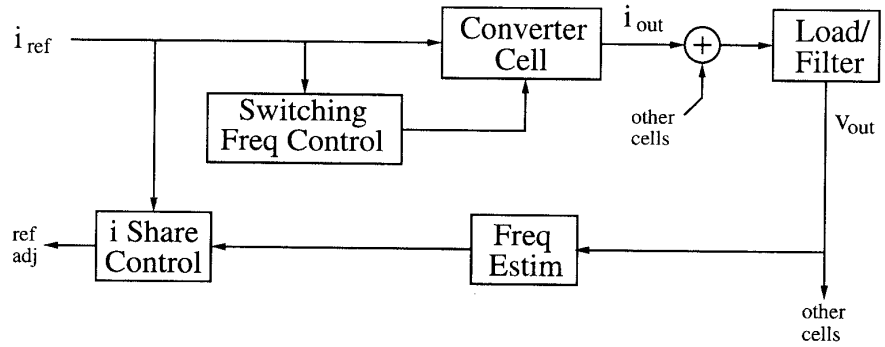

Figure 4 Schematic of the switching-frequency implementation of frequency-based load-sharing control.

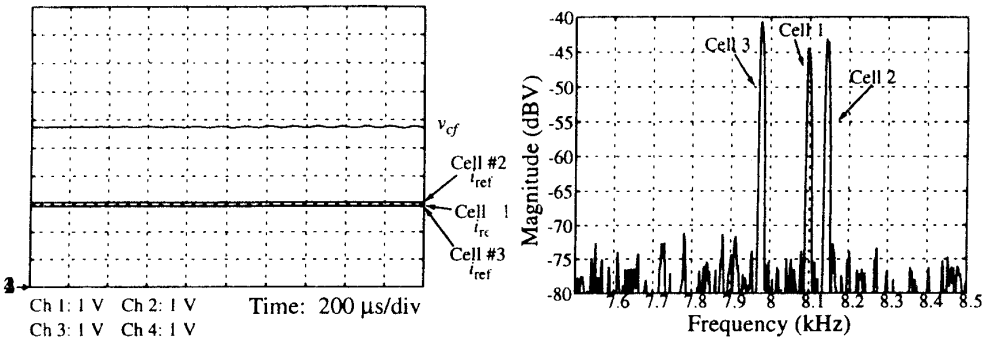

(a) (b)

Figure 5 Operation of the prototype parallel converter system at approximately 50% load. (A) System output voltage and cell reference currents. (B) Spectrum of the output voltage perturbations used to achieve current sharing.

operating under current-mode control with nominal input and output voltages of 15V and 5V, respectively. Each cell has a perturbation generator circuit which implements an incrementally linear relationship between cell reference current and perturbation frequency. Cell currents from no load to full load (25 mA) yield cell perturbation frequencies from 5 to 10 kHz. The perturbation frequency range is selected to be well above the output voltage control bandwidth of the system, but well below the 200 kHz cell switching frequency. The perturbation magnitude is proportional to the perturbation frequency (to compensate for the capacitive output filter) and its range is selected to yield very small (<1%) output voltage ripple. The system employs the rms frequency estimator structure of Fig. 1, with the averaging time constants of the rms-to-dc converters chosen to be faster than the current-sharing loop bandwidth, but slower than the other system time constants. Further details about the prototype system design and its evaluation can be found in [25].

Figure 5a shows the cell reference currents and output voltage of the prototype system at approximately 50 percent of full load, while Fig. 5b shows the spectrum of the output voltage perturbations used to achieve current sharing. For this load, the cell currents are balanced to within 3% of their average and the output voltage ripple is below 1%, while without current-sharing control the same load yields a 2:1 current imbalance between the highest and lowest cell currents. Figure 6 shows the static current-sharing behavior of the system over the whole load range, while Fig. 7 shows the current-sharing dynamics for 10% to 90% load steps. What may be concluded from these results is that the frequency encoding method can be used to achieve accurate static and dynamic current sharing among paralleled converters without interconnections among cells for current sharing.

V. CONCLUSIONS

This paper has presented a new method for achieving current-sharing among paralleled converters, based on frequency encoding of the needed information. The current-sharing approach has been analyzed, and different implementation methods have been described. We have shown that the new approach has significant advantages over existing methods, including the ability to galvanically isolate or eliminate the current-sharing connections among cells and the freedom to select the frequency range over which information is communicated. The design of a low-power experimental prototype has been presented, along with experimental results demonstrating the practicality of the method. This converter system achieves very accurate current-sharing using very simple load-sharing circuitry and with no additional interconnections among cells.

In conclusion, we would like to point out that other approaches to current-sharing are possible which are similar to those presented here and which share some of the same advantages. For example, encoding and communicating current-sharing information on the *amplitudes* of *fixed-frequency* (and phase) signals can be employed to achieve galvanic isolation of current-sharing control circuits. Alternatively, frequency encoding of variables other than current or use of other estimation and control structures may be desirable for some applications. It may be expected that frequency-encoding and similar approaches to current sharing will have advantage whenever fault tolerance and high reliability are important system requirements.

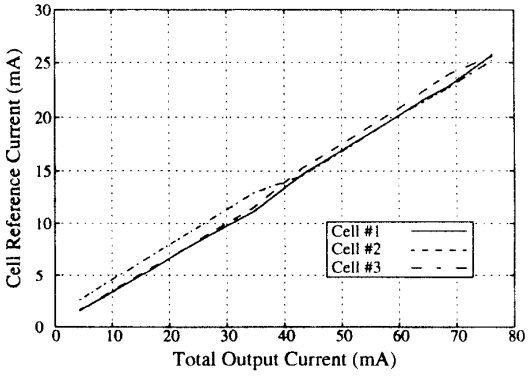

Figure 6 Converter cell reference currents vs. total output current illustrating the static current-sharing capability of the prototype system.

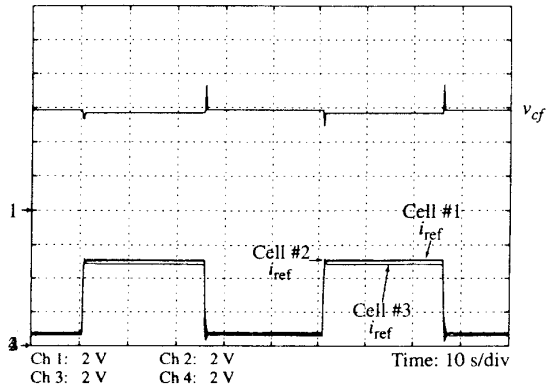

Figure 7 Current-sharing dynamics of the prototype system for 10% - 90% load steps.

ACKNOWLEDGMENTS

The authors would like to gratefully acknowledge support for this research from the Bose Foundation. Generous equipment grants from the Intel and Tektronix Corporations facilitated this research and are greatly appreciated. David Perreault gratefully acknowledges support from an IEEE Convergence Fellowship in Transportation Electronics, and Robert Selders thanks Delco Electronics for support through the DE Scholarship Program.

APPENDIX A: RMS-TO-DC CONVERSION

This appendix addresses the application of practical rms-to-dc converters to the computations outlined in the paper. Most integrated circuit rms-to-dc converters either explicitly or implicitly calculate the rms of a signal *f(t)* as

$$f_{rms}(t) = \sqrt{LPF\{f^2(t)\}} \tag{6}$$

where *LPF* denotes a low-pass filtering operation, typically using a first or second order filter. We will focus on the effects of computing the mean square using this technique; the rms value is merely the square root of this. We define the weighted mean square of a signal *f(t)* with respect to a weighting (or windowing) function *w(t)* as

$$f_{wms} = \frac{\int_{-\infty}^{\infty} [w(\tau)\, f(\tau)]^2 d\tau}{\int_{-\infty}^{\infty} w(\tau)^2 d\tau} . \tag{7}$$

For the conventional mean square value f_{ms}, we use the weighting function

$$w_T(\tau) = \begin{cases} 1 & -\frac{T}{2} < \tau < \frac{T}{2} \\ 0 & otherwise \end{cases} \tag{8}$$

and take the limit as $T \to \infty$, which yields

$$f_{ms} = \lim_{T\to\infty} \frac{1}{T} \int_{-\frac{T}{2}}^{\frac{T}{2}} f(\tau)^2 d\tau . \tag{9}$$

Now consider calculating the "computed mean square" of a signal *f(t)* using a first-order butterworth filter with time constant τ_1. This filter has an impulse response

$$h(t) = \frac{1}{\tau_1} e^{-t/\tau_1} u(t) \tag{10}$$

which yields a computed mean square of *f(t)*

$$\begin{aligned} f_{cms}(t) &= f^2(t) * h(t) \\ &= \frac{1}{\tau_1} \int_{-\infty}^{t} e^{(\tau - t)/\tau_1} f^2(\tau) d\tau \\ &= \frac{1}{\tau_1} \int_{-\infty}^{\infty} [e^{(\tau - t)/(2\tau_1)} u(t - \tau) f(\tau)]^2 d\tau \end{aligned} \tag{11}$$

Examining the form of the last line of **(11)**, it is easily shown that $f_{cms}(t)$ is equivalent to the weighted mean-square computation **(7)**, with weighting function

$$w_c(\tau) = e^{(\tau - t)/(2\tau_1)} u(t - \tau) . \tag{12}$$

The fact that the weighting function is zero for values of τ greater than t makes physical sense, since computations in the actual circuit can only be based on past values of the input signal. This weighting function places a weight of one on the present value of the input signal, with weights for past times decaying exponentially to zero with time constant $2\tau_1$. Thus, the longer the time constant $2\tau_1$, the more heavily the past values of the input signal are weighted, and the slower the system responds to changes in the input.

The impact of computing the mean square as in **(11)** can also be examined from a frequency resolution point of view. This is important, since mean-square computations in the frequency-encoding method are typically made on signals composed of closely-spaced discrete frequency components. Applying Parseval's relation to **(7)**, we find

$$f_{wms} = \frac{1}{(2\pi)^2 E_w} \int_{-\infty}^{\infty} |W(j\omega) * F(j\omega)|^2 d\omega \tag{13}$$

where E_w is the energy in the weighting function *w(t)*. From the frequency domain point of view, the mean square reflects the true content of $F(j\omega)$ to the extent that its content is not changed by convolution with $W(j\omega)$. The Fourier transformation of the conventional weighting function from **(8)**, $W_T(j\omega)$, is a sinc

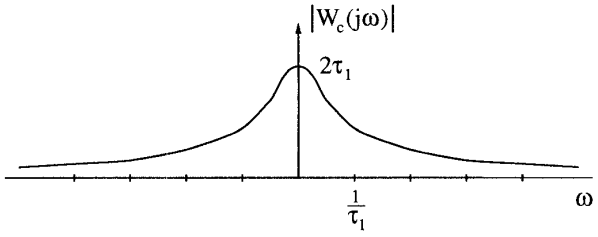

Figure 8 Frequency response magnitude plot for the weighting function of **(12)**.

function with mainlobe width $\Delta\omega = 2\pi/T$. Thus, the conventional mean-square calculation accurately reflects the spectral content of $f(t)$ to within a resolution of approximately $2\pi/T$, and resolves frequencies with arbitrary accuracy as $T \to \infty$.

We now consider practical computation of the mean square using the weighting function of **(12)**, which has the transform

$$W_c(j\omega) = \frac{2\tau_1 e^{-j\omega t}}{1 - j2\tau_1\omega} \qquad \textbf{(14)}$$

where τ is treated as time, and t is a constant parameter. The magnitude of this weighting function frequency response is plotted in Fig. 8. From this, we see that the effect of the weighting function is to "smear" the spectral content of $F(j\omega)$ by an amount depending on τ_1. There will be significant overlap and loss of resolution among spectral components of $F(j\omega)$ which are closer than roughly $3/\tau_1$ to $5/\tau_1$ apart. The spectral smearing caused by the weighting function affects the computation of the mean square, and limits the frequency resolution of a practical estimator.

Thus, practical rms-to-dc converters of the type **(6)** allow changes in spectral content to be tracked across time, while limiting the frequency resolution of the computation. Both tracking response speed and frequency resolution are controlled by the filter time constant τ_1, and must be traded off against one another in the design process. Similar design issues can be expected to arise in other approaches to the problem, such as with the use of higher order filters or with discrete-time implementations of the mean-square computation.

REFERENCES

[1] M. Hashii, K. Kousaka, and M. Kaimoto, "New Approach to a High Power PWM Inverter for AC Motor Drives", *IEEE Industry Applications Society Annual Meeting*, 1985, pp. 467-472.

[2] H. Huisman and B. Gravendeel, "A Modular and Versatile Control Method for Phase-Staggering Multiple Power Converters", *European Power Electronics Conference*, pp. 959-963, 1989.

[3] K. Siri, C. Lee, and T. Wu, "Current Distribution Control for Parallel Connected Converters: Part I", *IEEE Trans. on Aerospace and Electronic Systems*, Vol. 28, No. 3, July, 1992, pp. 829-840.

[4] F. Petruzziello, P. Ziogas, and G. Joos, "A Novel Approach to Paralleling of Power Converter Units with True Redundancy", *IEEE Power Electronics Specialists Conference*, 1990, pp. 808-813.

[5] J. Holtz, W. Lokzat, and K. Werner, "A High-Power Multitransistor-Inverter Uninterruptible Power Supply System", *IEEE Transactions on Power Electronics*, Vol. 3, No. 3, July 1988, pp. 278-285.

[6] J. Holtz and K. Werner, "Multi-Inverter UPS System with Redundant Load Sharing Control", *IEEE Transactions on Power Electronics*, Vol. 37, No. 6, Dec. 1990, pp. 506-513.

[7] J. Chen and C. Chu, "Combination Voltage-Controlled and Current-Controlled PWM Inverters for UPS Parallel Operation", *IEEE Transactions on Power Electronics*, Vol. 10, No. 5, Sept. 1995.

[8] S. Okuma, K. Iwata, and Katsuaki Suzuki, "Parallel Running of GTO PWM Inverters", *IEEE Power Electronics Specialists Conference*, 1984, pp. 111-120.

[9] J.G. Kassakian, "High Frequency Switching and Distributed Conversion in Power Electronic Systems," *Sixth Conference on Power Electronics and Motion Control (PEMC 90)*, Budapest, 1990.

[10] J.G. Kassakian and D.J. Perreault, "An Assessment of Cellular Architectures for Large Converter Systems," *First International Conference on Power Electronics and Motion Control*, Beijing, 1994, pp. 70-79.

[11] D. Perreault, J. Kassakian, and H. Martin, "A Soft-Switched Parallel Inverter Architecture with Minimal Output Magnetics," *1994 IEEE Power Electronics Specialists Conference*, Taipei, 1994, pp. 970-977.

[12] L. Walker, "Parallel Redundant Operation of Static Power Converters," *IEEE Industry Applications Society Annual Meeting*, 1973, p. 603-614.

[13] T. Kawabata and S. Higashino, "Parallel Operation of Voltage Source Inverters," *IEEE Transactions on Industry Applications*, Vol. 24, No. 2, Mar/Apr 1988, pp. 281-287.

[14] K.T. Small, "Single Wire Current Share Paralleling of Power Supplies," *U.S. Patent 4,717,833*, 1988.

[15] R. Wu, T. Kohama, Y. Kodera, T. Ninomiya, and F. Ihara, "Load-Current-Sharing Control for Parallel Operation of DC-to-DC Converters," *IEEE Power electronics Specialists Conference*, 1993, pp. 101-107.

[16] T. Kohama, T. Ninomiya, M. Shoyama, and F. Ihara, "Dynamic Analysis of Parallel Module Converter System with Current Balance Controllers," *1994 IEEE Telecommunications Energy Conference Record*, 1994, pp. 190-195.

[17] V.J. Thottuvelil and G.C. Verghese, "Stability Analysis of Paralleled DC/DC Converters with Active Current Sharing," *IEEE Power Electronics Specialists Conference*, 1996, (in press).

[18] M. Youn and R. Hoft, "Analysis of Parallel Operation of Inverters," *IEEE Industry Applications Society Annual Meeting*, 1976, pp. 951-958.

[19] D. Maliniak, "Dense DC-DC Converters Actively Share Stress," *Electronic Design*, Jan. 21, 1993, pp. 39-44.

[20] M. Jordan, "UC3907 Load Share IC Simplifies Parallel Power Supply Design", *Unitrode Application Note U-129*, Unitrode Corp., Merrimack, NH.

[21] M. Chandorkar, D. Divan, and R. Adapa, "Control of Parallel Connected Inverters in Stand-Alone AC Supply Systems," *IEEE Industry Application Society Annual Meeting*, 1991, pp. 1003-1009.

[22] J. Bocek and C. Liu, "Determining Current Sharing Criterion for Parallel Operation of Power Converters in Multi-Module Bus Systems," *IEEE Power Electronics Specialists Conference*, 1990, pp. 870-879.

[23] J. Glaser and A. Witulski, "Output Plane Analysis of Load-Sharing in Multiple-Module Converter Systems," *IEEE Transactions on Power Electronics*, Vol. 9, No. 1, Jan. 1994, pp. 43-50.

[24] R.V. White and F.M. Miles, "Principles of Fault Tolerance," *IEEE Applied Power Electronics Conference*, 1996, pp. 18-25.

[25] R.L. Selders, "A Current-Balancing Control System for Cellular Power Converters", S.M. Thesis, *M.I.T. Department of Electrical Engineering and Computer Science*, Feb. 1996.